

Supporting Information

Compositional Engineering of Doped Zero-dimensional Zinc Halide Blue Emitters for Efficient X-ray Scintillation

Yingchun Zhou¹, Quan Zhou¹, Xiaowei Niu¹, Zheng-Guang Yan^{1}, Taifeng Lin², Jiawen*

Xiao^{1} and Xiaodong Han¹*

1-Institute of Microstructure and Property of Advanced Materials, Beijing Key Lab of Microstructure and Property of Advanced Materials, Faculty of Materials and Manufacturing, Beijing University of Technology, Beijing 100124, China

2-Faculty of Environment and Life, Beijing University of Technology, Beijing 100124, China

E-mail: yanzg@bjut.edu.cn; xiaojw@bjut.edu.cn; xdhan@bjut.edu.cn

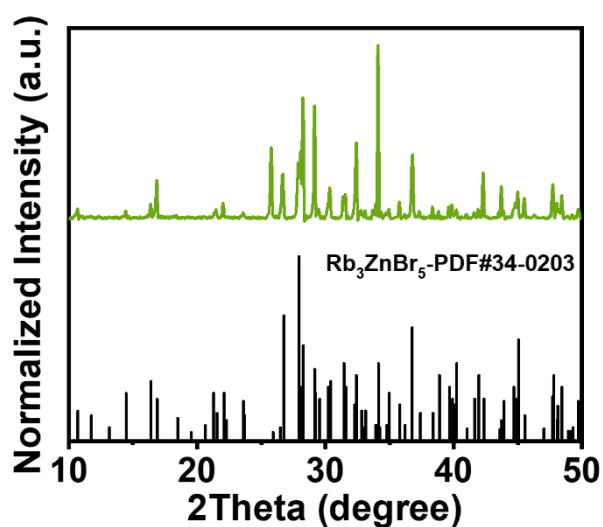
Table S1. Composition of Cu-doped samples measured by ICP-AES.

samples	Cu/Zn precursors ratio	Cu content (at%, ICP)
Cu-doped Cs ₂ ZnBr ₄	2/3	0.67
	3/3	36
	4/3	65
	5/3	103
	6/3	140
Cu-doped Cs ₂ ZnCl ₄	2/3	0.30
Cu-doped Rb ₂ ZnCl ₄	2/3	0.59

$$\text{Cu/Zn precursors ratio} = \frac{\text{molar feed ratio of CuBr}}{\text{molar feed ratio of ZnBr}_2}$$

The content of Cu was expressed relative to that Zn, which was assumed to be 1.

$$\text{Cu content} = \frac{\text{Cu concentration measured by ICP}}{\text{Zn concentration measured by ICP}} \times 100\%$$

**Figure S1.** XRD pattern of Rb₃ZnBr₅.

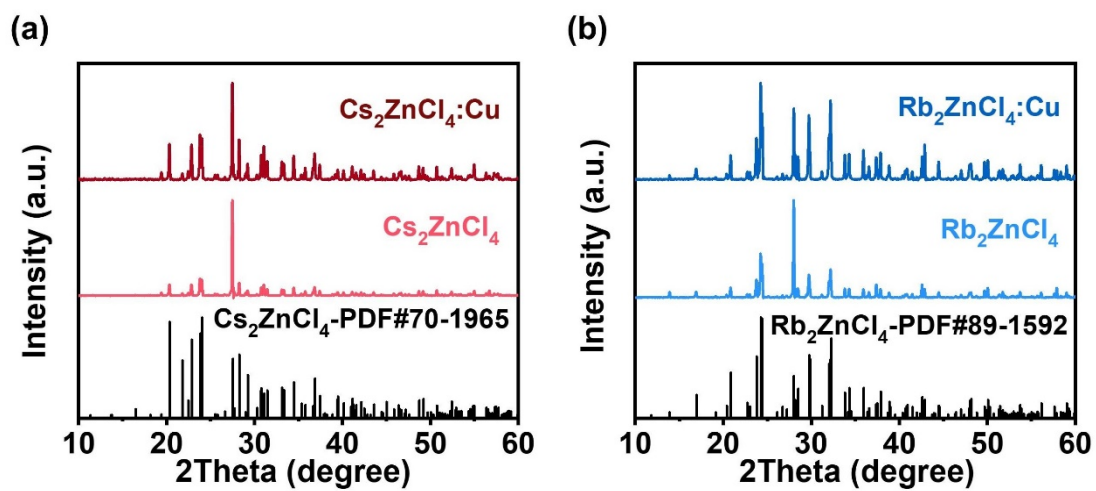


Figure S2. (a) XRD patterns of pristine Cs₂ZnCl₄ and Cs₂ZnCl₄:Cu. (b) XRD patterns of pristine Rb₂ZnCl₄ and Rb₂ZnCl₄:Cu.

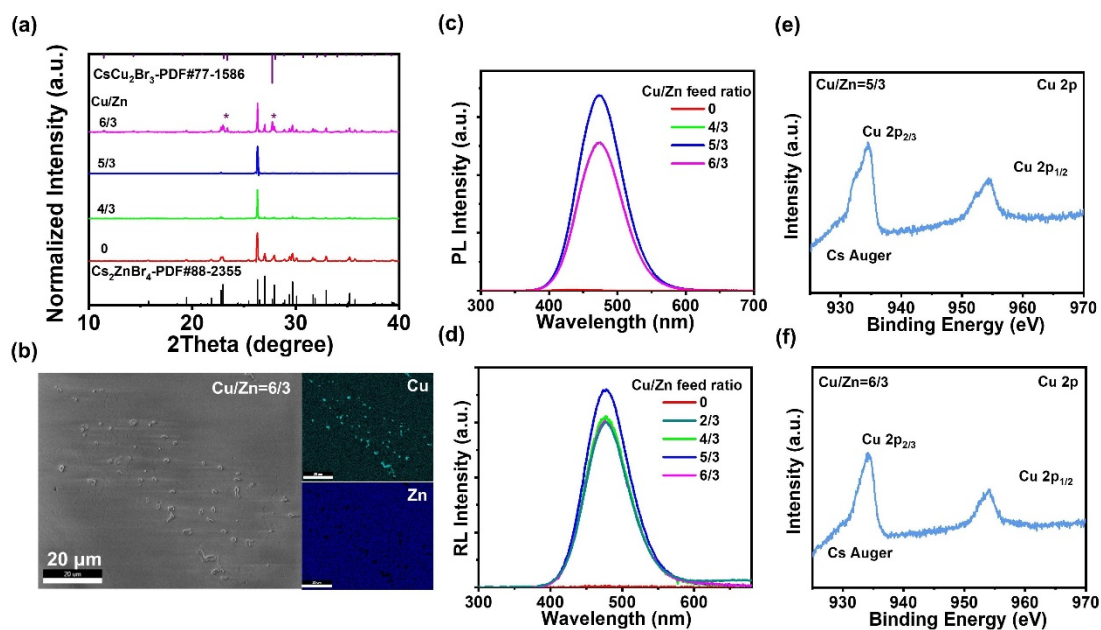


Figure S3. (a) XRD patterns of pristine Cs₂ZnBr₄ and Cu-doped Cs₂ZnBr₄ with different Cu to Zn precursors ratio. (b) SEM image and the element distribution analysis through EDS mapping of the as-prepared Cu-doped Cs₂ZnBr₄ single crystals with Cu/Zn precursors ratio of 6/3 (Scale bar: 20 μm). (c) The PL spectra of pristine Cs₂ZnBr₄ and Cu-doped Cs₂ZnBr₄ with different Cu to Zn precursors ratio. (d) The RL spectra of pristine Cs₂ZnBr₄ and Cu-doped Cs₂ZnBr₄ with different Cu to Zn molar feed ratio. (e) High-resolution XPS spectrum of Cu 2p for Cu-doped Cs₂ZnBr₄ single crystals with Cu/Zn precursors ratio of 5/3 and (f) 6/3.

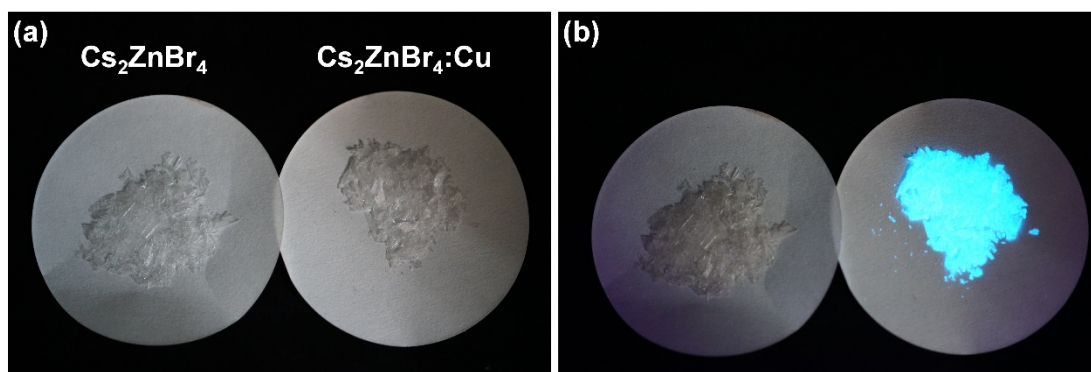


Figure S4. (a) The photographs of Cs_2ZnBr_4 and $\text{Cs}_2\text{ZnBr}_4:\text{Cu}$ under room light. (b) The photographs of Cs_2ZnBr_4 and $\text{Cs}_2\text{ZnBr}_4:\text{Cu}$ under 254 nm UV.

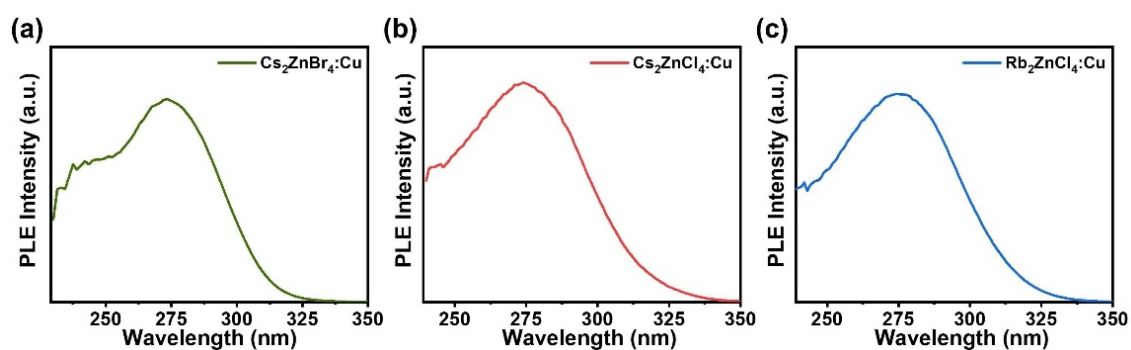


Figure S5. PLE spectra of $\text{Cs}_2\text{ZnBr}_4:\text{Cu}$, $\text{Cs}_2\text{ZnCl}_4:\text{Cu}$ and $\text{Rb}_2\text{ZnCl}_4:\text{Cu}$.

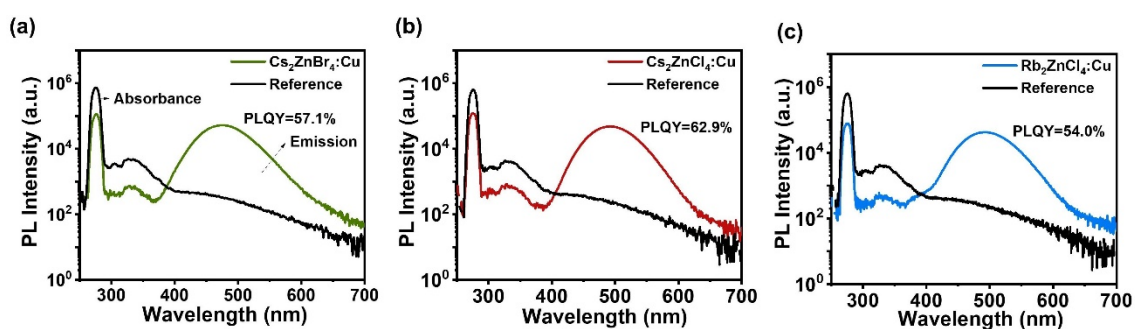


Figure S6. Absolute PL quantum yield (PLQY) measurement results of $\text{Cs}_2\text{ZnBr}_4:\text{Cu}$, $\text{Cs}_2\text{ZnCl}_4:\text{Cu}$ and $\text{Rb}_2\text{ZnCl}_4:\text{Cu}$.

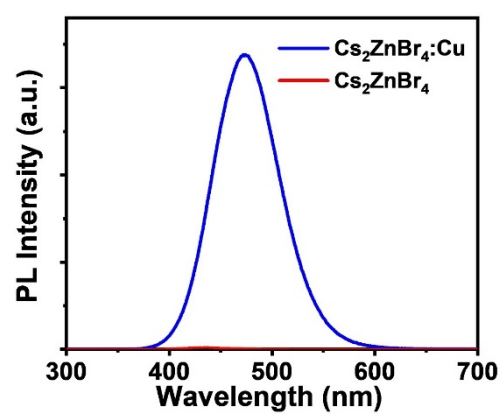


Figure S7. The PL spectra of Cs_2ZnBr_4 and $\text{Cs}_2\text{ZnBr}_4:\text{Cu}$.

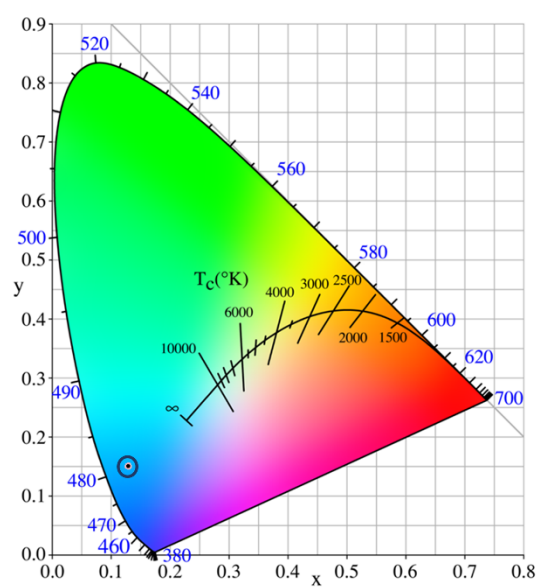


Figure S8. The CIE (International Commission on Illumination) diagram of $\text{Cs}_2\text{ZnBr}_4:\text{Cu}$. (0.1326,0.1458).

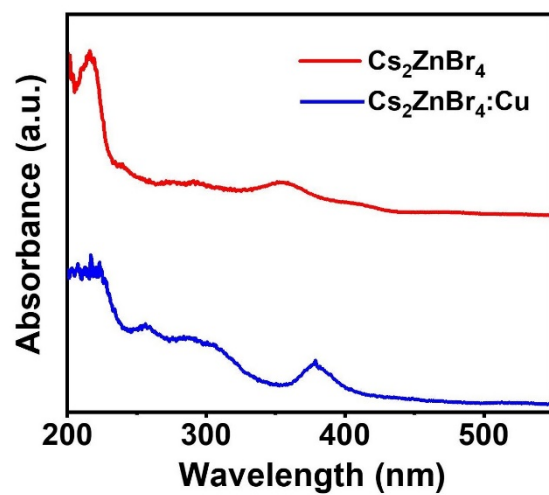


Figure S9. The UV-vis absorption spectra of Cs_2ZnBr_4 and $\text{Cs}_2\text{ZnBr}_4:\text{Cu}$.

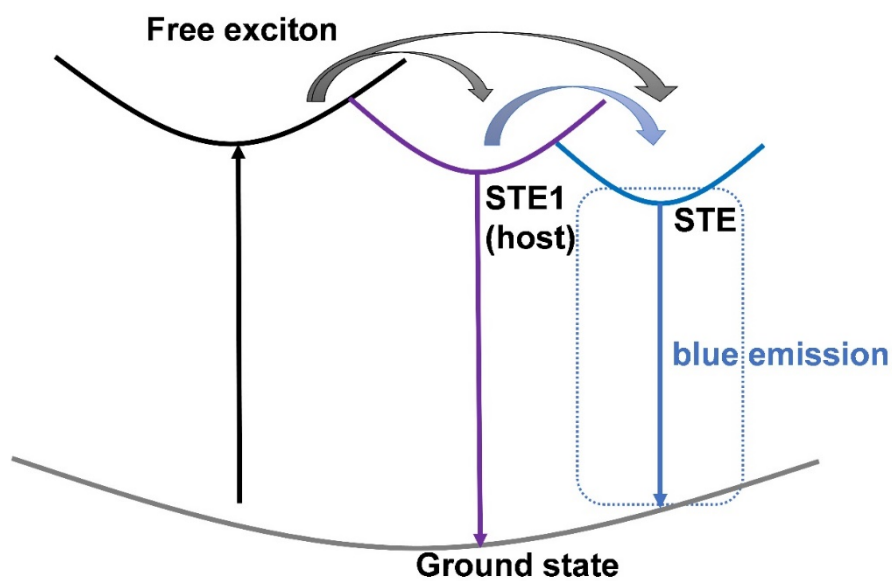


Figure S10. Schematic illustration of photophysical processes of the pure-blue emission in $\text{Cs}_2\text{ZnBr}_4:\text{Cu}$.

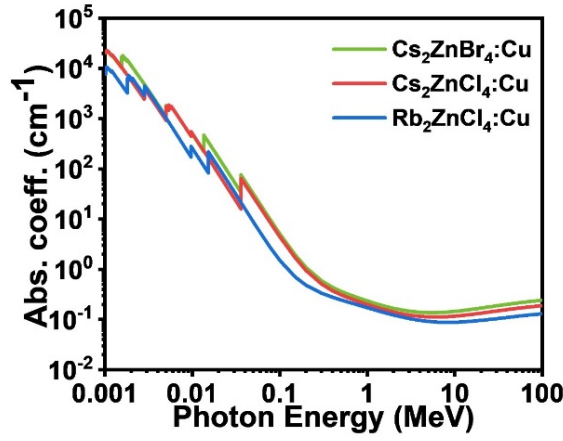


Figure S11. X-ray absorption coefficients of $\text{Cs}_2\text{ZnBr}_4\text{:Cu}$, $\text{Cs}_2\text{ZnCl}_4\text{:Cu}$ and $\text{Rb}_2\text{ZnCl}_4\text{:Cu}$ as a function of photon energy from 1 keV to 100 MeV.

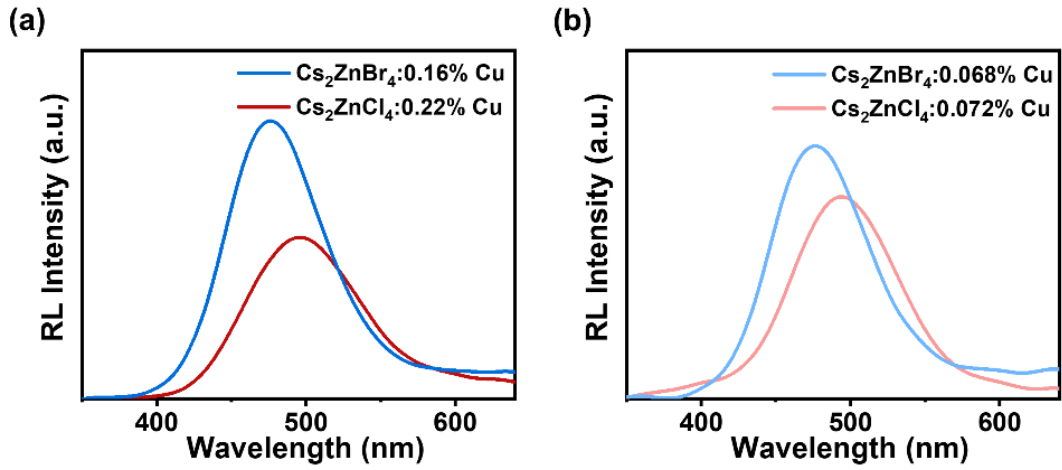


Figure S12. RL spectra of Cu-doped Cs_2ZnBr_4 and Cu-doped Cs_2ZnCl_4 samples with similar Cu content. RL spectra of Cu-doped Cs_2ZnBr_4 and Cu-doped Cs_2ZnCl_4 samples with (a) the relatively higher and (b) the relatively lower Cu content.

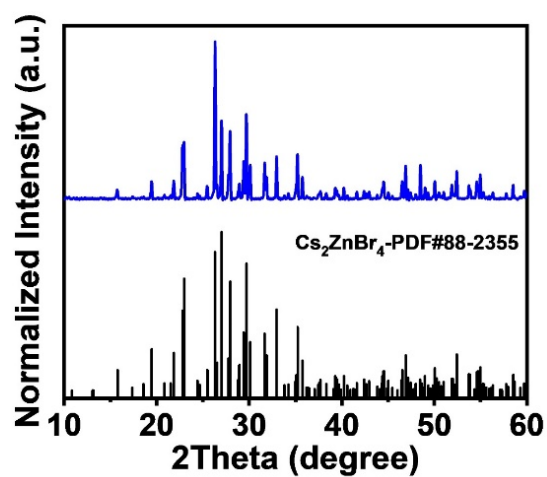


Figure S13. XRD pattern $\text{Cs}_2\text{ZnBr}_4\text{:Cu}$ after storing in ambient atmosphere for four months.

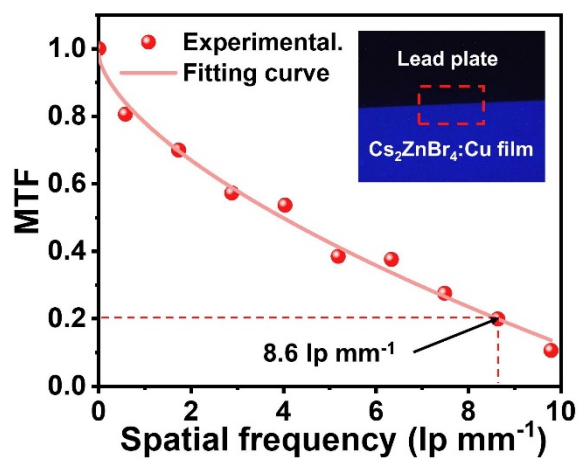


Figure S14. Modulation transfer function (MTF) curve of $\text{Cs}_2\text{ZnBr}_4\text{:Cu}$ film.